Qian, Jianfeng, Izquierdo, Benito, Gao, Steven, Wang, Hanyang, Zhou, Hai and Xu, Huiliang (2024) *A Novel Low-Cost H-plane Decoupling Technique for Two Closely Placed Patch Antennas Using Electric and Magnetic Coupling Cancellation.* IEEE Transactions on Antennas and Propagation . ISSN 1558-2221.

A Novel Low-Cost Decoupling Technique for Two Closely Placed Patch Antennas Using Electric and Magnetic Coupling Cancellation

Jianfeng Qian, Benito Sanz Izquierdo, Steven Gao, *Fellow*, *IEEE*, Hanyang Wang, *Fellow*, *IEEE*, Hai Zhou, and Huiliang Xu

Abstract— **This paper presents a novel low-cost method for decoupling two closely-placed patch antennas. This new decoupling concept is simple yet highly effective, requiring no additional decoupling structures or complicated manufacturing processes. According to the proposed concept, the mutual coupling between two patches can be suppressed by controlling the weight of electric (*E*) and magnetic (*H*) coupling between them. When the *E*-coupling and *H*-coupling are comparable, a deep null will arise on the mutual coupling curve, resulting in a high isolation in the band of interest. To validate the approach, two prototypes for both 2-element and 4-element multi-input multi-output (MIMO) arrays, are designed, fabricated, and measured. The experimental results agree well with the simulations, highlighting the advantages of this method, including low cost, high isolation, and simpler antenna structures.**

*Index Terms—***Cancellation, closely placed, decoupling, MIMO, patch antenna.**

I. INTRODUCTION

AS one of the most popular antenna type, the patch antenna is widely used in many applications for its low cost, planar structure, low profile, and ease of fabrication. In a modern communication system, multiple antennas are integrated on the same printed circuit board for higher capacity or diversity purpose. However, the mutual coupling problem is always a bottleneck which limits the final achievable system performance. High mutual coupling can not only deteriorate the total efficiency of the system, but also reduce the overall capacity. In extreme cases, the energy transmitted from one antenna to another can even damage the receiving transceiver.

To mitigate the mutual coupling between two patch antennas, extensive research has been conducted over the years. One common approach to improve the isolation is by reducing the surface wave coupling [1-5]. This concept is widely used when the patches are placed within a relatively large distance, where the surface wave dominates the mutual coupling. Alternatively, the mutual coupling can also be reduced by introducing a band-reject response in the band of interest by using inter-patch loading elements, such as resonators [6], [7] and slot structures [8-10]. Additionally, the mutual coupling can be reduced by changing the coupling mode between the patches using structures such as near-field resonators [11] and polarization conversion isolator [12]. Networks introducing another path to cancel the mutual coupled field is also a good option for mutual coupling reducing [13-17]. However, all these designs either need additional space for the implementation of decoupling structures or suffers from large antenna separations.

Some simple yet effective methods without using any additional decoupling structures is achieved by studying the natural field characteristics of patch antennas [18-20]. By intentionally designing antenna structures and arrangements, isolation between antenna ports can be achieved, offering the advantages of low cost and ease of fabrication.

This paper focuses on a specific scenario where two antennas are closely placed. It is well-known that as the distance between antenna elements decreases, the mutual coupling between them increases, particularly when they are in the same polarization. Additionally, the close proximity of the patches makes it challenging to implement complex decoupling structures between them.

In [9], two patch antennas are decoupled by cutting a resonating slot on the finite ground plane. This slot effectively traps the energy that would have coupled from one antenna to the other, resulting in improved isolation. However, this structure is sensitive to the ground plane size and may lead to high backside radiation [10]. Furthermore, cutting a slot on the ground is not ideal for many practical applications as it may interfere with devices mounted on the other side of the system board. In [11], closely packed patches are decoupled using an additional near-field resonating layer over the patches. With an edge-to-edge separation of 0.024 wavelength at the center frequency, 20 dB isolation is achieved. In [14], the mutual coupling between two closely placed patches is achieved by a simple metal strip coupled to both patches. This coupled strip introduces an additional out-of-phase coupling path between the two antenna ports. With an edge-to-edge distance of 0.027 λ_0, the mutual coupling between the two ports is reduced to -18 dB. Unfortunately, the final achieved bandwidth is only 1.43%. In [20], two extremely closely placed patches are decoupled by making the patches operating over the higher order modes. At the cost of slightly reduced bandwidth and longer patch, a simple physical offset in the polarization

J. F. Qian and Benito Sanz Izquierdo are with the School of Engineering and Digital Arts, University of Kent, Canterbury CT2 7NT, U.K. (e-mail: jq42@kent.ac.uk).

Steven Gao is with the Chinese University of Hongkong, Hong Kong.

H. Zhou and H. Wang are with Huawei Technology Ltd., Reading RG2 6UF, U.K.

(a)

(b)

Patches
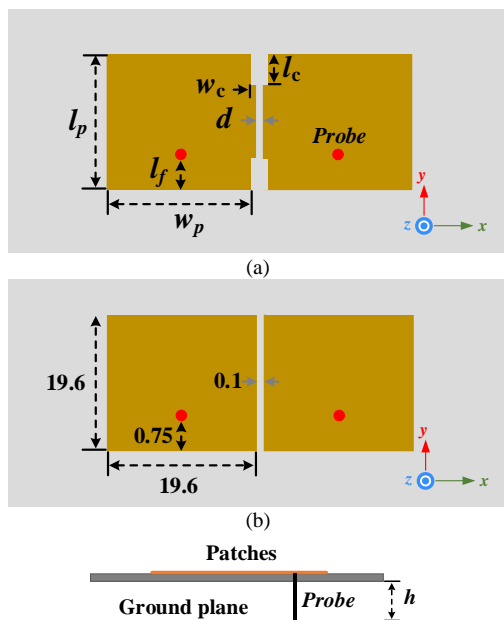
Ground plane | *Probe* | *h*

Fig. 1. Structure of the proposed decoupled patch antennas. (a) decoupled patch antennas. (b) reference design of coupled antennas with dimensions in mm. (c) side view. Dimensions in mm: l_f = 1.45, l_p = 21, l_c = 5, w_c = 0.2, w_p = 22, d = 0.1, h = 3.

Fig. 2. Simulated responses for the reference design and proposed decoupled antennas.

Fig. 3. Prototype of the proposed MIMO array.

direction can significantly improve the isolation up to 20 dB in the band of interest even when the antenna separation is only 0.007 λ_0 at its center frequency. A mode cancellation method is presented in [21] to reduce the mutual coupling between two closely packed patches. However, the presented examples only show isolations in the level of about 15 dB. In addition, for mutli-element MIMO scenarios, dummy patches are required to ensure a symmetric environment for the outer patches.

Up to now, most state-of-the-art decoupling techniques for closely packed antennas involve the use of additional decoupling structures [7]-[11], [14], [21], [22] or require extra space [20] for implementation. Some of them also suffer from small bandwidths which are limited by the quality factors of resonant structures adopted in the decoupling process [9-11], [14]. To ensure a compact form factor, short design flow, and low cost, it is crucial to develop a simpler yet effective decoupling technique specifically for closely packed patch antennas.

In this paper, a novel decoupling technique for two extremely closely placed patch antennas is presented. The decoupling of the proposed technique is based on the field analysis of the fundamental mode of a patch antenna. By cutting different regions at the non-radiating edges, the weight of electric and magnetic couplings between patches is adjusted. Then, it is found that the mutual coupling can be significantly reduced in the operating band by simply changing the dimensions of the cuts. Compared to other presented decoupling architectures, the proposed technique does not need any additional decoupling elements or complicated fabrication processes. To validate the effectiveness of our technique, we provide two example designs: one for a 2-element array and another for a 4-element multi-input multi-output (MIMO) array. Through our study, the proposed technique has the following advantages:
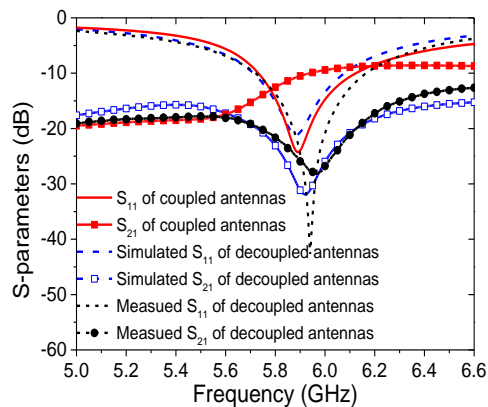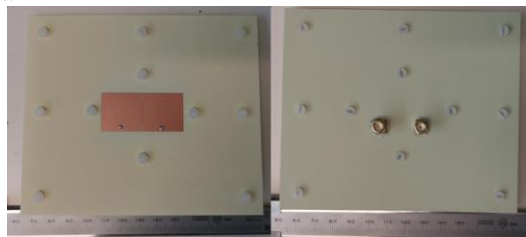
1) It is capable of dealing with extremely small antenna separation.

2) No additional decoupling element or complicated manufacturing process is needed, which means a simple structure, ease of fabrication, ease of design, and cost-efficient.

3) Small effect on the antennas' radiation performance, which means it is suitable for array applications too.

4) The theory can also be extended to MIMO arrays with multiple elements.

The paper starts with the design of a dual-antenna MIMO array. The performance of the 2-element MIMO is discussed first. Based on this structure the mechanism of the proposed technique is studied in Section II-C. Then, according to the decoupling mechanism, design philosophy of the technique is explained together with some parametric studies in Section II-D. Afterwards, the concept is extended to 4-element MIMO array in Section III. The performance of the proposed decoupling technique is also compared to other presented works in this section. Finally, Section IV draws a conclusion.

II. COUPLING MECHANISM BETWEEN PATCH ANTENNAS

A. Antenna Structure

Figure 1(a) depicts the physical structure of the proposed decoupled antennas, illustrating two patches placed in extremely close proximity. The distance between the two patches is set to 0.1 mm. The antennas are fed by a metal probe with radius of 0.35 mm. The substrate employed in this design is Roger 4003, with a dielectric constant of 3.55 and a thickness of 0.3 mm. Notably, Fig. 1(a) shows only two modified patch antennas without any additional decoupling elements. The only modification applied to the antennas involves cuts made at their corners. The specific design rules to decide the patch dimensions will be elaborated upon in the next few sections.
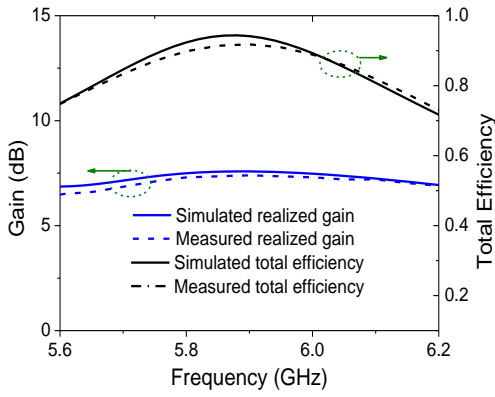
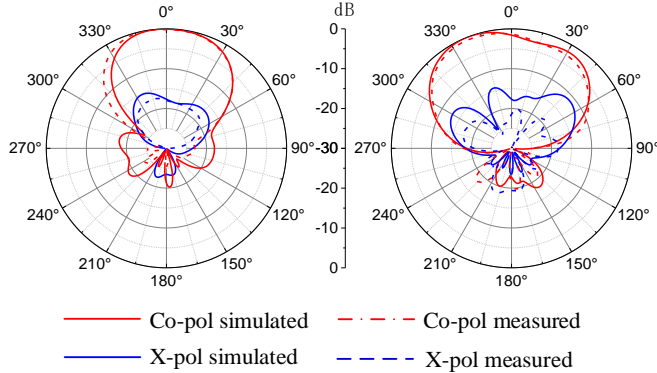Fig. 4. Simulated and measured gain and efficiency of the antennas.

Fig. 5. Simulated and measured radiation patterns at the center frequency.

B. Antenna Performance

According to classical antenna theory, the mutual coupling between patch antennas is closely associated with the separation distance between them [23-26]. As the antennas are placed in closer proximity, the mutual coupling becomes stronger. In cases where the patches are positioned in an extremely small vicinity of each other, the mutual impedance has a significant impact on the impedance response of the coupled antennas.

First, a reference design without any decoupling process is simulated. The dimensions of the reference design are outlined in Fig. 1(b). In this reference design, two patches are strongly coupled, as illustrated by the response plotted in Fig. 2. The antennas operate at a center frequency of 5.9 GHz over their fundamental TM_{10} modes. Consequently, the total lengths of the patches in the Y-direction are approximately half-wavelength at 5.9 GHz. The edge-to-edge distance between the patches is 0.1 mm, which corresponds to 0.0018 λ_0 at the antenna's center frequency.

Without any modifications to the rectangular patches, the two antennas exhibit strong coupling, resulting in a low isolation of only 6.8 dB within their operating band when arranged at a distance of 0.1 mm. This strong coupling implies that a significant amount of energy will be consumed by one antenna when the other antenna is transmitting.

For the verification of the effect of the proposed novel decoupling concept, a prototype of the decoupled patch antennas is fabricated and measured with its photograph shown in Fig. 3. The simulated and measured S-parameters for the proposed decoupled antennas are presented in Fig. 2. The measured -10-dB bandwidth is 5.72 GHz to 6.16 GHz, while
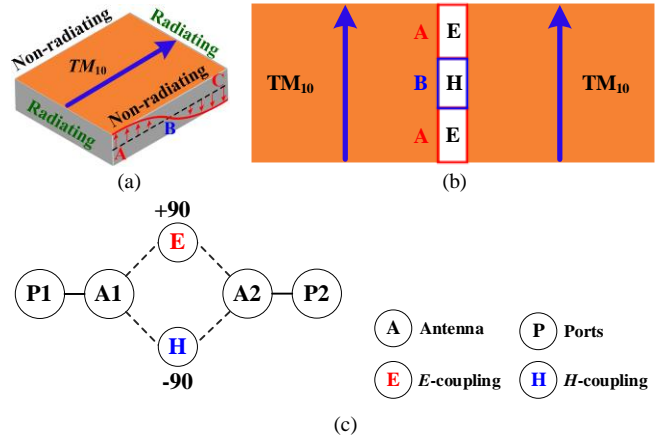
Fig. 6. (a) Electric field distribution under the patch for its fundamental TM_{10} mode, (b) coupling behaviour between two patch antennas. (c) topology for the coupled patch antennas.

the simulated bandwidth ranges from 5.71 GHz to 6.08 GHz. The center frequency of the operating band exhibits a slight shift towards the higher frequency range due to fabrication errors.

Using the proposed decoupling technique, the measured mutual coupling between the two antennas reduced to 18.7 dB. The only change to the proposed MIMO compared to the reference design is introducing some simple cuts at the patches' corners. With such a small change, a deep null is observed in the transmission curve of the decoupled antennas in Fig. 2, leading to a substantial improvement in isolation of up to 19.8 dB at the center frequency, compared to the coupled reference design.

Fig. 4 illustrates the simulated and measured gain and efficiency of the antennas. During the measurement process, one antenna is measured while the other one remains terminated with a 50-Ohm load. As the entire structure is symmetric, only one antenna measurement is required. The measured realized gain is 7.42 dBi, closely aligning with the simulated value of 7.57 dBi. The measured total efficiency exceeds 77% within the whole operating band, with S_{11} less than -10 dB. The peak total efficiency reaches 91%.

Fig. 5 shows the simulated and measured radiation patterns of the proposed decoupled antennas. Due to the structural symmetry, only one antenna is measured, while the other inactive antenna is terminated with a 50-Ohm wideband load. Broadside radiation is observed in both planes. The simulated and measured radiation patterns agree well. For both planes, the measured cross-polarization is lower than -16.7 dB and -18.3 dB, respectively. Because of the integrity of the ground plane, the antennas show good directional radiation for both planes. The measured front-to-back ratio is higher than 24.8 dB and 18.2 dB for E-plane and H-plane, respectively.

C. Decoupling Mechanism

To gain insight into the physical behavior of this structure, it is important to study the electric field distribution for the TM_{10} mode. Fig. 6 illustrates the electric field distribution beneath the patch for its non-radiating edges. As known, the TM_{10} mode exhibits a half-wavelength standing wave field distribution at its two non-radiating edges. The electric field reaches its peak at the open ends of the patch (regions A and
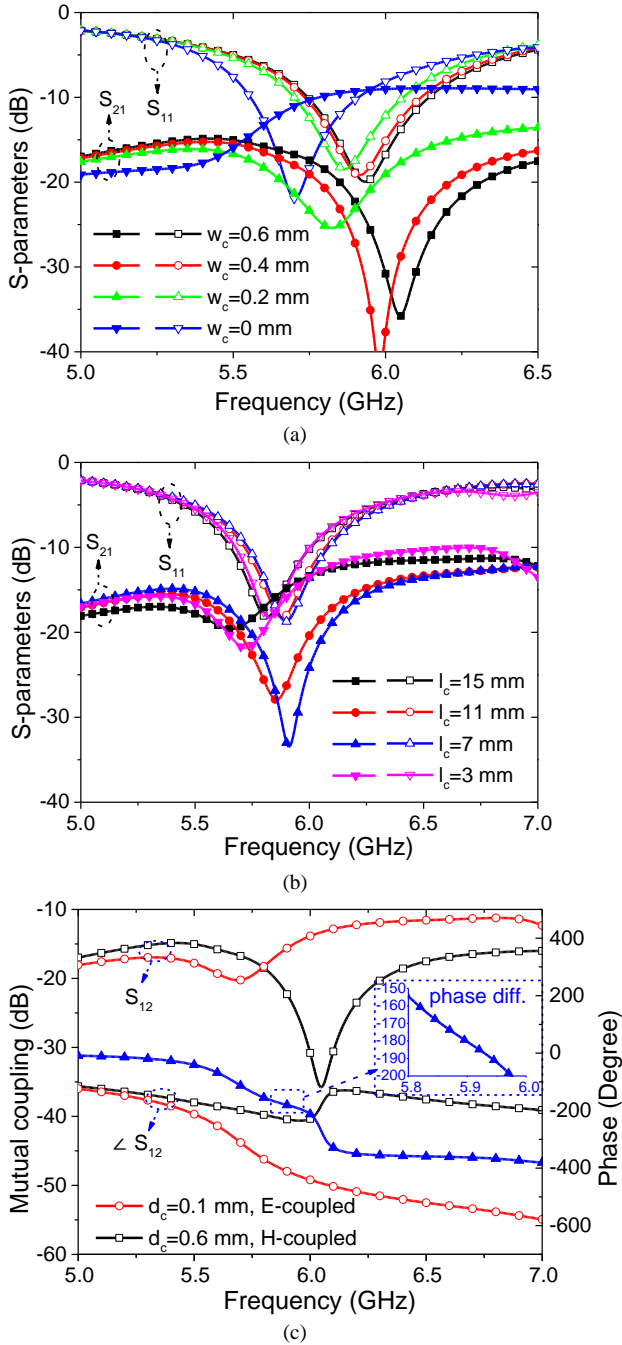
Fig. 7. Responses for the antennas with different (a) cut depths, (b) cut lengths, and (c) phase responses of the mutual couplings for *E*-coupled and *H*-coupled patches.

C), while it drops to a minimum at the center (region *B*). Conversely, a strong magnetic field distribution occurs at the virtually shorted center of the patch (region *B*), while it weakens at the open ends (regions *A* and *C*).

When two patches are positioned in close proximity, they will be strongly coupled through the electric (*E*) and magnetic (*H*) near fields, as depicted in Fig. 6 (b). Through our study, it is found that when the separation between the patches is extremely small, the electric field dominates the mutual coupling. To mitigate the *E*-coupling, the four corners of the patch (regions *A* and *C*) are cut, effectively moving the electric field beneath the patches away from each other. By doing so,

the *E*-coupling can be reduced while the weight of the *H*-coupling can be increased consequently. Within a certain tuning range, the *E*- and *H*-couplings become comparable in the antennas' operating band. In this specific scenario, the two coupling mechanisms cancel each other out, resulting in a low level of mutual coupling.

This behavior can be explained by the fact that electric and magnetic couplings always possess opposite signs when they coexist within the same network as shown in Fig. 6 (c) [27-29]. This characteristic is commonly utilized in filter designs to control the positions of transmission zeros (TZs). In this work, the theory is borrowed to minimize the coupling between two patches. In filter designs, TZs are typically positioned at out-of-band frequencies to improve selectivity. However, for effective decoupling performance in antennas, the TZs must be located within the antennas' operating bands. To accomplish this, the electric and magnetic couplings should have the same magnitude. Consequently, the cuts on the patches need to be carefully designed.

D. Parametric study

In order to provide a better understanding of the design philosophy behind the proposed decoupling technique, several key parameters are investigated in this section using Ansys High-Frequency Structure Simulator (HFSS). It is important to note that when studying one parameter, the remaining parameters are kept at the values specified in Fig. 1.

First, the most important parameter which affects the decoupling performance is the depth of the cut on the patch. The frequency responses for the dual-patch module with different cut depths are simulated and provided in Fig. 7 (a). When there is no cut on the patch, namely $w_c = 0$, the two patches are electrically coupled, resulting in a high transmission level between the antenna ports. According to the theory mentioned in [27], electric-coupled patches exhibit a TZ below the operating band.

As the edges of the patch are modified and the cut depth increases, the electric coupling decreases while the magnetic coupling becomes dominant. This leads to a gradual frequency shift of the TZ to higher frequencies [27]. By carefully designing the cut depth, the transmission zero can be positioned near the resonances of the antennas, resulting in a deep null in the transmission coefficient and achieving a high isolation.

Another factor affecting the coupling behaviour between two patches is the length of the cut on the patch (l_c). A parametric sweep is done on the cut length (l_c) with the simulated results provided in Fig. 7 (b). The curves indicate that when the cut is very short ($l_c = 3$ mm), the transmission zero is located at a lower frequency band compared to the antenna's resonance frequency. As the cut length increases ($l_c = 7$ and 11 mm), the transmission zero shifts to higher frequencies. However, when the cut length exceeds an even larger value ($l_c = 15$ mm), the transmission zero moves back to the lower frequency band.

This phenomenon can be explained by studying the field distributions illustrated in Fig. 6. The electric field in regions *A* and *C* is very high, so even a small variation in the cut length has a significant effect on the coupling strength related to the electric field. As the cut length increases, the electric field
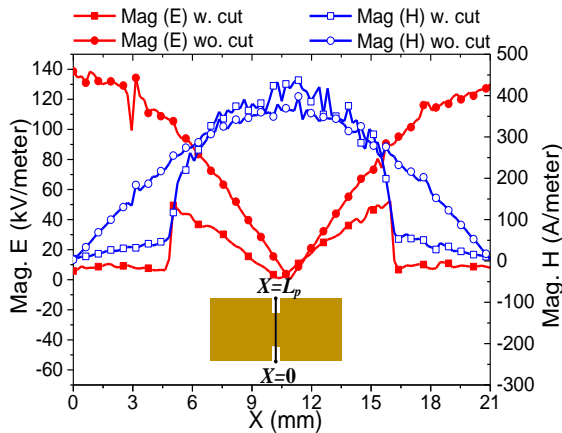
Fig. 8. Simulated *E* and *H* field distributions along the coupled edge.

Fig. 9. Structure photograph (not available now) of the 4-element MIMO array. Dimensions in mm: $l_{f1} = 1.05$, $l_{p1} = 20.4$, $l_{c1} = 4.65$, $l_{f2} = 0.6$, $l_{p2} = 20.4$, $l_{c2} = 5.65$, $w_{c1} = w_{c2} = 0.12$, $w_{p1} = 23.9$, $w_{p2} = 26.1$, $d_1 = 0.85$, $d_2 = 1.45$.

Fig. 10. Prototype of the proposed 4-element MIMO array.

(a)

(b)

Fig. 11. Simulated and measured *S*-parameters for the 4-element MIMO array (a) reflection coefficients. (b) isolations.

strength decreases, causing the transmission zero to shift to higher frequencies. However, when the cut reaches region B, further increasing the cut length weakens the *H*-coupling more than the *E*-coupling. Consequently, with a very long cut ($l_c = 15$ mm), the magnetic coupling may become smaller than the electric coupling again, leading to the dominance of the electric coupling mechanism. This results in the TZ moving back to the lower frequency band in terms of *S*-parameters. From this parametric study, an important design rule can be derived: the cut should be designed with an appropriate length. An excessively long cut can deteriorate the decoupling performance, so it is crucial to optimize the cut length to achieve the desired coupling characteristics. According to the authors' experience, a cut length smaller than one-third of the patch length is recommended.

In addition to the previous studies, another important parametric study for the phase response of the mutual coupling is carried out to further reinforcing the validity of the proposed decoupling concept. The results are presented in Fig. 7 (c). Two cases are studied here. In the first case, where the electric coupling dominates, a shallow cut (red line with $d_c = 0.1$ mm) is implemented. Conversely, in the second case, the patches are magnetically coupled with a deeper cut (black line with $d_c = 0.6$ mm).

When the patches are electrically coupled, the TZ is at the lower frequency band. When the patches are magnetically coupled, the TZ is at the higher frequency band. The phase responses of the two cases exhibit distinct trends at the resonance frequency of the patch. Notably, the difference between the phases (*phase diff.*) is calculated and plotted. As can be seen, the phase difference approaches approximately 180 degrees near the resonance frequency of the patch (5.9 GHz). This phenomenon provides strong evidence that supports the proposed decoupling concept in Section II-C.

E. Field distributions

To gain a deeper understanding of the proposed decoupling concept, the field distributions at the non-radiating edges, where the coupling occurs, are investigated. Specifically, the electric (*E*, represented by red lines) and magnetic (*H*, represented by blue lines) field distributions are analyzed. Fig. 8 depicts the field magnitudes along a line between two patches for two different cases: one with unmodified patches (strongly coupled) and the other with decoupled patches.

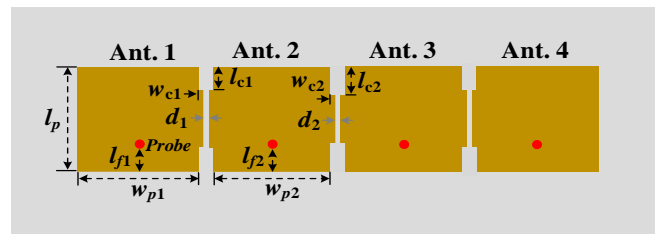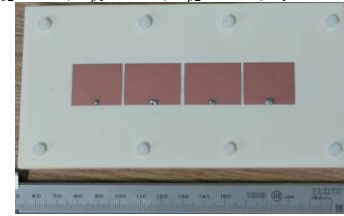In the case of strongly coupled patches without any
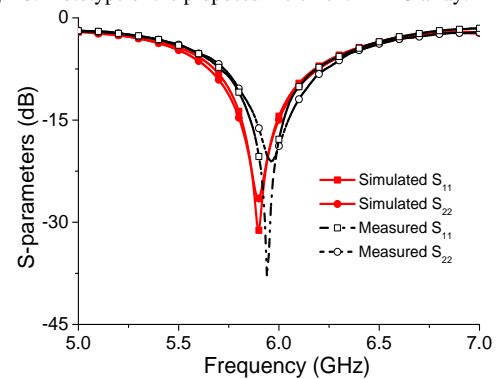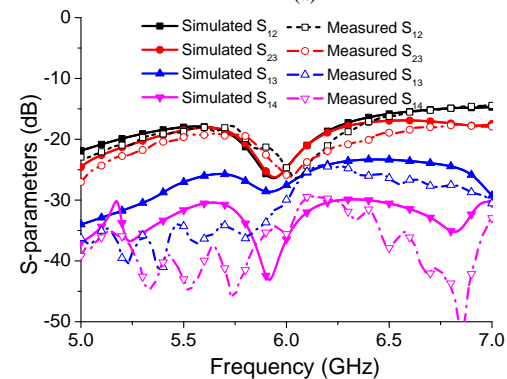
modification, the electric and magnetic fields exhibit the behaviors described in Section II-C. Strong electric field density can be observed at the regions where *X*=0 mm - 4.5 mm and *X*=16.5 mm - 21 mm, which corresponds to the two open-ends of the patches. When the patches' corners are cut, the field density at the open ends is significantly reduced. This reduction is more significant for the electric field because the *H*-field is inherently weak at the open ends. Since the fringing electric field at the non-radiating edges is weak, the magnitude of the electric field at these edges is significantly reduced when the mutual coupling is decreased, as shown in Fig. 8.

The field distributions depicted in Fig. 8 provide insight

Table I.
Comparison of the performance between different works in the literature and this work.

Reference	Decoupling scheme	Design complexity	Additional space for decoupling	Antenna type	Isolation improvement (dB)	Number of the element	Edge-to-edge distance (λ_0)	Isolation (dB)	Bandwidth
[9]	Resonant slot on the ground	Normal	Yes	Patch	Not given	2	0.031	30	1.7%
[10]	Slot on the ground	Normal	Yes	Inverted-F antenna	13.7	2	0.009	20	4.1%
[11]	Stacked near-field resonators	Complex	Yes (Extra layer)	Patch	10	2/8	0.016/0.028	20/20	1.4%/0.4%
[14]	Co-planar resonator	Complex	Yes	Patch	11	2	0.02	18	1.43%
[20]	Higher-order mode operation	Normal	Yes	Patch	12	2 / 4	0.007 / 0.02	20.2/21.5	4%/3.6%
[21]	Inductors	Multiple steps	Yes (Dummy patches)	Patch	10.4/7.2	2/4	0.016	15.4/12.2	5.5%/3.5%
This work	Modified patches	Simple	NO	Patch	11.9	2	0.0018	18.7	7.4%
						4	0.026	19.3	6%

into the underlying physical reality of the proposed decoupling concept. The cuts at the ends of the non-radiating edges have a stronger effect on the electric coupling, allowing for separate control of the electric and magnetic coupling.

III. FOUR-ELEMENT MIMO ARRAY

A. Four-Element MIMO Array

The proposed decoupling concept can also be easily extended to the design of larger-scale MIMO arrays. For demonstration, a four-element MIMO array is designed with the same stack-up as the previous 2-element one. The structure of the four-element MIMO array is depicted in Fig. 9, where the four patches are positioned along their *H*-plane. Following the design concept introduced in the section II, the corners of the patches are all modified. Due to the asymmetric environment for the first antenna (ant.1) and fourth antenna (ant. 4), these two antennas are designed with slightly different dimensions from the other two antennas at the outer sides (ant. 2 and ant. 3). The dimension of the structure is provided in Fig. 9. The antenna is fabricated and measured. Fig. 10 presents a photograph of the fabricated antenna.

The simulated and measured responses of the four-element MIMO array are presented in Fig. 11. The measured -10 dB bandwidths for ant.1 and ant.2 are 5.78 GHz – 6.1 GHz and 5.79 GHz - 6.14 GHz, respectively, while the simulated results indicate bandwidths of 5.72 GHz – 6.08 GHz and 5.74 GHz - 6.09 GHz, respectively. Within their respective -10 dB bandwidths, the minimum isolation between ant.1 and ant.2 is 19.3 dB. Specifically, the measured isolations between adjacent patches are 19.3 dB (S_{12}) and 20.1 dB (S_{23}), which correspond to simulated values of 19.1 dB and 19.5 dB, respectively. The isolations between non-adjacent patches are 25 dB (S_{13}) and 29 dB (S_{14}), with corresponding simulated values of 26 dB and 32 dB, respectively. In terms of the reflection coefficients, the simulations and measurements exhibit good agreement, despite minor differences in resonance frequencies that can be attributed to fabrication errors. The isolation curves for adjacent elements agree well, while slight variations in the isolation curves for non-adjacent elements can be attributed to the sensitivity of low-magnitude
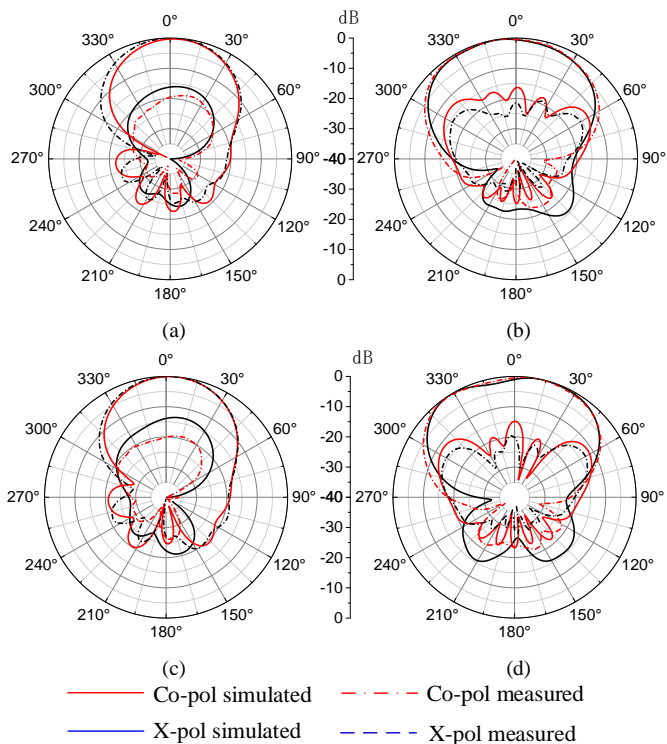

(a)

(b)

(c)

(d)

——— Co-pol simulated   – · – · – Co-pol measured
——— X-pol simulated   – – – – X-pol measured

Fig. 12. Radiation patterns for the 4-element MIMO array. (a) *E*-plane with ant. 1 excited. (b) *H*-plane with ant. 1 excited. (c) *E*-plane with ant. 2 excited. (d) *H*-plane with ant. 2 excited.

transmission coefficients to the surrounding environment in a multi-antenna module.

Simulated and measured radiation patterns of the fabricated 4-element MIMO are presented in Fig. 12. Two cases are measured here. Generally, broadside radiaton patterns can be observed for both cases. Because no modification is introduced to the ground plane, for all the cases, the antenans show front-to-back ratio of higher than 20 dB. Besides, as only small changes are done to the geometry of the patchs, good TM_{10} mode radiation is perserved for all the antennas. Thus, all these antennas show low cross-polarizations. More specifically, when ant. 1 is activated whereas the other antenans are terminated with 50-Ohm loads, the measured corss-polarization levels are 18.8 dB and 19 dB lower than the co-polarization for the *E*- and *H*-planes,

respectively. For the ant.2, the cross-polarization levels are higher than 19.4 dB and 19.6 dB in the broadside direction for the *E*- and *H*-planes, respectively.

B. Comparison and discussion

In the table I, the performance of the proposed designs is compared to other presented works. First, the proposed decoupling technique shows the simplest structure without using any additional decoupling structure [9]-[11], [14]., additional layer [11], or increase antenna area [20]. Some of these presented designs also suffers from time-consuming design process. In contrast, our proposed method has an extremely simple design flow. From the parametric studies carried out in the Section II-D, designers only need to pay attention to two key parameters during the decoupling process.

Secondly, the proposed 2-element MIMO design achieves the smallest antenna separation which is only 0.002 free-space wavelength. For the isolation level, the proposed technique ensures a general mutual coupling up to 18.7 dB within the band-of-interest, with an isolation improvement of 11.9 dB. Although the isolation performance in [9] is higher than this value, the decoupling method in [9] requires a long slot on the ground plane. Besides, the decoupling ability of this resonating slot is very sensitive to the ground size. These limitations make it not suitable for applications where system ground plane integrity is important.

The proposed concept is also verified effective for both 2-element and 4-element MIMO arrays. Regarding the specific design example presented in this paper, the proposed method shows the widest decoupling bandwidth compared to other presented works. Some decoupling techniques requires resonating structure to accomplish reduced mutual coupling in the band of interest. Nevertheless, a resonant structure always shows frequency-relevant impedance characteristic, which means that these decoupling structures may only work well in a limited frequency range. This explains why some decoupled antennas show very narrow impedance bandwidths [9]-[11], [14].

Considering the size, fabrication complexity, decoupling ability, and antenna separation, the proposed technique provides a very attractive decoupling solution for small-separation multi-antennas system.

IV. CONCLUSION

This paper presents a novel decoupling solution for patch antennas positioned in extremely close proximity. The proposed technique eliminates the need for additional decoupling structures or layers by introducing very simple modifications to the patch structure itself. The effectiveness of the concept is demonstrated through the design and analysis of both 2-element and 4-element MIMO arrays. Comparative evaluations against existing state-of-the-art decoupling techniques highlight several advantages of the proposed method, including its simplicity in structure, cost-effectiveness, and suitability for applications requiring minimal antenna separation. In summary, the proposed decoupling solution offers a promising approach to address the mutual coupling challenges in closely placed patch antennas, showing promising application prospects in various wireless communication systems for enhanced performance and improved system integration.

REFERENCES

[1] E. Rajo-Iglesias *et al.*, "Mutual coupling reduction in patch antenna arrays by using a planar ebg structure and a multilayer dielectric substrate," *IEEE Transactions on Antennas and Propagation,* vol. 56, no. 6, pp. 1648-1655, 2008.

[2] Y. Fan, and Y. Rahmat-Samii, "Microstrip antennas integrated with electromagnetic band-gap (ebg) structures: A low mutual coupling design for array applications," *IEEE Transactions on Antennas and Propagation,* vol. 51, no. 10, pp. 2936-2946, 2003.

[3] S. Ghosal *et al.*, "Analysis and reduction of mutual coupling in a microstrip array with a magneto-electric structure," *IEEE Transactions on Electromagnetic Compatibility,* vol. 63, no. 5, pp. 1376-1383, 2021.

[4] A. Askarian *et al.*, "Surface-wave control technique for mutual coupling mitigation in array antenna," *IEEE Microwave and Wireless Components Letters,* vol. 32, no. 6, pp. 623-626, 2022.

[5] J.-G. Yook, and L. P. B. Katehi, "Micromachined microstrip patch antenna with controlled mutual coupling and surface waves," *IEEE Transactions on Antennas and Propagation,* vol. 49, no. 9, Sept. 2001.

[6] K. S. Vishvaksenan *et al.*, "Mutual coupling reduction in microstrip patch antenna arrays using parallel coupled-line resonators," *IEEE Antennas and Wireless Propagation Letters,* vol. 16, pp. 2146-2149, 2017.

[7] A. Habashi *et al.*, "Mutual coupling reduction between very closely spaced patch antennas using low-profile folded split-ring resonators (FSRRS)," *IEEE Antennas and Wireless Propagation Letters,* vol. 10, pp. 862-865, 2011.

[8] C.-Y. Chiu *et al.*, "Reduction of mutual coupling between closely-packed antenna elements," *IEEE Transactions on Antennas and Propagation,* vol. 55, no. 6, pp. 1732-1738, 2007.

[9] J. OuYang *et al.*, "Reducing mutual coupling of closely spaced microstrip mimo antennas for wlan application," *IEEE Antennas and Wireless Propagation Letters,* vol. 10, pp. 310-313, 2011.

[10] S. Zhang *et al.*, "Mutual coupling reduction of two pifas with a t-shape slot impedance transformer for mimo mobile terminals," *IEEE Transactions on Antennas and Propagation,* vol. 60, no. 3, pp. 1521-1531, 2012.

[11] M. Li *et al.*, "Isolation enhancement for mimo patch antennas using near-field resonators as coupling-mode transducers," *IEEE Transactions on Antennas and Propagation,* vol. 67, no. 2, pp. 755-764, 2019.

[12] Y.-F. Cheng *et al.*, "Reduction of mutual coupling between patch antennas using a polarization-conversion isolator," *IEEE Antennas and Wireless Propagation Letters,* vol. 16, pp. 1257-1260, 2017.

[13] J. Andersen, and H. Rasmussen, "Decoupling and descattering networks for antennas," *IEEE Transactions on Antennas and Propagation,* vol. 24, no. 6, pp. 841-846, November 1976.

[14] T. Pei *et al.*, "A low-profile decoupling structure for mutual coupling suppression in mimo patch antenna," *IEEE Transactions on Antennas and Propagation,* vol. 69, no. 10, pp. 6145-6153, 2021.

[15] Y.-M. Zhang *et al.*, "A wavetrap-based decoupling technique for 45° polarized mimo antenna arrays," *IEEE Transactions on Antennas and Propagation,* vol. 68, no. 3, pp. 2148-2157, 2020.

[16] Y.-M. Zhang *et al.*, "A simple decoupling network with filtering response for patch antenna arrays," *IEEE Transactions on Antennas and Propagation,* vol. 69, no. 11, pp. 7427-7439, 2021.

[17] L. Zhao *et al.*, "A novel second-order decoupling network for two-element compact antenna arrays," *2012 Asia Pacific Microwave Conference Proceedings*, pp. 1172-1174, Dec. 2012.

[18] Q. X. Lai *et al.*, "Mutual coupling reduction in mimo microstrip patch array using tm10 and tm02 modes," *IEEE Transactions on Antennas and Propagation,* vol. 69, no. 11, pp. 7562-7571, 2021.

[19] H. Lin *et al.*, "Weak-field-based self-decoupling patch antennas," *IEEE Transactions on Antennas and Propagation,* vol. 68, no. 6, pp. 4208-4217, 2020.

[20] J.-F. Qian *et al.*, "Mutual coupling suppression between two closely placed patch antennas using higher order modes," *IEEE Transactions on Antennas and Propagation*, pp. 1-1, 2023.

[21] L. Sun *et al.*, "Decoupling between extremely closely spaced patch antennas by mode cancellation method," *IEEE Transactions on Antennas and Propagation,* vol. 69, no. 6, pp. 3074-3083, 2021.

[22] Y. Xin Mi *et al.*, "Reduction of mutual coupling between closely packed patch antennas using waveguided metamaterials," *IEEE Antennas and Wireless Propagation Letters,* vol. 11, pp. 389-391, 2012.

[23] H. King, "Mutual impedance of unequal length antennas in echelon," *IRE Transactions on Antennas and Propagation,* vol. 5, no. 3, pp. 306-313, July 1957.

[24] N. Alexopoulos, and I. Rana, "Mutual impedance computation between printed dipoles," *IEEE Transactions on Antennas and Propagation,* vol. 29, no. 1, pp. 106-111, Jan. 1981.

[25] A. Derneryd, "A theoretical investigation of the rectangular microstrip antenna element," *IEEE Transactions on Antennas and Propagation,* vol. 26, no. 4, pp. 532-535, Jul. 1978.

[26] D. Pozar, "Input impedance and mutual coupling of rectangular microstrip antennas," *IEEE Transactions on Antennas and Propagation,* vol. 30, no. 6, pp. 1191-1196, Nov. 1982.

[27] J.-F. Qian *et al.*, "A novel electric and magnetic gap-coupled broadband patch antenna with improved selectivity and its application in mimo system," *IEEE Transactions on Antennas and Propagation,* vol. 66, no. 10, pp. 5625-5629, 2018.

[28] J.-S. Hong, and M. J. Lancaster, "Couplings of microstrip square open-loop resonators for cross-coupled planar microwave filters," *Transactions on Microwave Theory and Techniques,* vol. 44, no. 12, Dec. 1996.

[29] J. B. Thomas, "Cross-coupling in coaxial cavity filters-a tutorial overview," *IEEE Transactions on Microwave Theory and Techniques,* vol. 51, no. 4, pp. 1368-1376, 2003.